

PAM/PEI polymer gel for water control in high-temperature and high-pressure conditions: Core flooding with crossflow effect

Zulhelmi Amir^{*,***,†}, Ismail Mohd Saaid^{**}, Badrul Mohamed Jan^{*,***}, Muhamad Fazly Abdul Patah^{*,***},
Munawar Khalil^{****}, and Wan Zairani Wan Bakar^{*****}

*Department of Chemical Engineering, Faculty of Engineering, Universiti Malaya, 50603 Kuala Lumpur, Malaysia

**Petroleum Engineering Department, Universiti Teknologi PETRONAS, 32610 Bandar Seri Iskandar,
Perak Darul Ridzuan, Malaysia

***Center for Energy Science, Universiti Malaya, 50603 Kuala Lumpur, Malaysia

****Department of Chemistry, FMIPA Universitas Indonesia, Kampus UI Depok, Depok 16424, Indonesia

*****Oil & Gas Department, School of Chemical Engineering, College of Engineering,
Universiti Teknologi MARA, 40450 Shah Alam, Selangor Darul Ehsan, Malaysia

(Received 14 July 2021 • Revised 15 October 2021 • Accepted 4 November 2021)

Abstract—Polymer gel has been established as a water shut-off control agent for improved oil recovery. The role of the polymer gel in conformance control is to divert injected water from high permeability to low permeability zones of the reservoir. This paper presents a series of core flooding tests performed to investigate the propagation, blocking capability, permeability reduction and diverting performance of various mixtures of polymer gels at simulated reservoir condition. In this particular study, a core flooding scheme with crossflow effect using composite core has permeability contrast. Core flooding test with crossflow effect simulates reservoirs with communication between reservoir permeability layers. Experimental results show that PAM/PEI polymer gel reinforced with solid silica NP has been proven to provide satisfactory gel strength to divert water flow, thus recovering an additional 24% of oil. This reinforced PAM/PEI polymer gel tends to recover more trapped oil compared to weakened PAM/PEI polymer gel without solid particles. These results give better understanding and provide additional knowledge of strengthening gel by addition of solid particles, which could be the remedy for the weakened polymer gel.

Keywords: Polymer Gel, Organic Crosslinker, Water Control, Core Flooding, Cross Flow

INTRODUCTION

Managing produced water is a great challenge for many oil and gas field operators. In 2014, worldwide daily water production was estimated at 310 million barrels from offshore and onshore oil fields, with 78 million barrels of oil per day [1]. This is equivalent to four barrels of water being brought up to the surface simultaneously with every barrel of oil. In fact, in certain mature regions in North America and the Middle East, the water to oil ratio can be as high as 10 to 14 [2,3]. According to these statistics, oil companies could turn their core business to water business. In addition, in terms of sheer volume, excessive water production is growing as rapidly as reservoir oil rates are declining. It also has been reported that the cost of disposing produced water is high. The cost can be as high as USD 5 per barrel of water, depending on the technology used for producing water disposal [1,4]. Taking USD 0.5 per barrel of water as the nominal disposal cost, the global oil and gas industry has to bear the huge amount of approximately USD 55 billion per year in managing 310 million barrels of water per day.

Reducing water production through conformance control has

gained much attention in the upstream oil and gas industry. Sydansk and Romero-Zeron define conformance control as a treatment to reduce excess water production throughout the recovery of oil [5]. Notwithstanding the stage of the oil recovery, whether primary production, secondary waterflooding or tertiary recovery, the proper design of conformance control increases the effectiveness and profitability from the particular oil and gas operation [6]. In this case, conformance control is conducted typically by reducing the permeability of the high permeability region of the reservoir [7,8]. Through permeability alteration, the new subsequent water injection will flow into the “higher permeability” zone where the leftover oil is located [9]. Chemical methods have been proven to be pertinent for most of the reservoirs that require conformance control by permeability reduction [10]. In-situ crosslinked polymer, in particular, have been widely deployed for several decades as blocking agents to reduce excessive water production [11-13].

In-situ crosslinked polymer gels are designed to propagate through fractures and layers with high permeability and high water saturation. It helps in creating a barrier to prevent water penetration and consequently to reduce the flow of unwanted water [12]. Seright et al. in 2012 established the concept of gel placement into reservoir to four stages [14]. First, injection of low viscosity gelant into the target zones. Second, water injection to push the low viscosity gel away from the wellbore. Then, shut-in well to allow gelation to occur

[†]To whom correspondence should be addressed.

E-mail: zulhelmi.amir@um.edu.my

Copyright by The Korean Institute of Chemical Engineers.

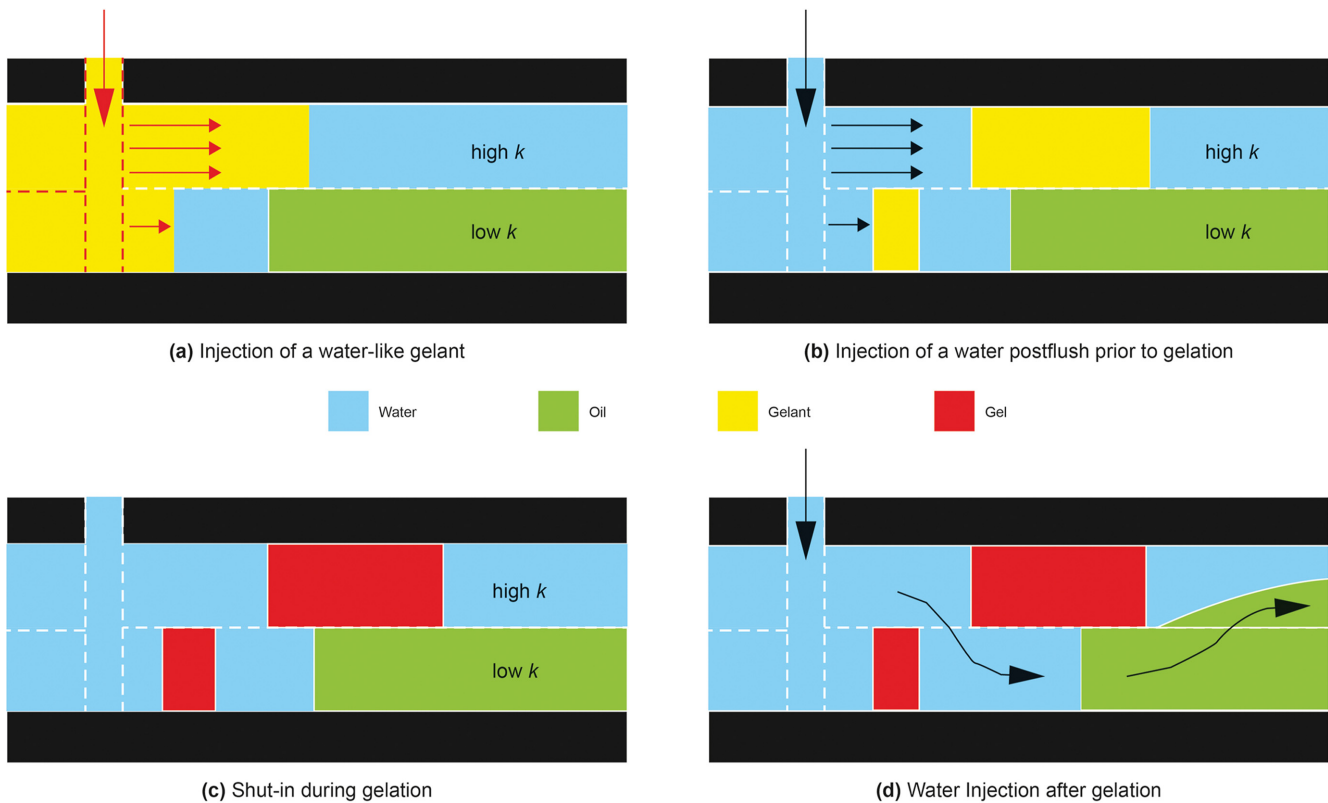


Fig. 1. The concept of placement and formation of gel for conformance control with crossflow effect. Figure from [15].

and polymer gelant turns into a rubber-like gel structure through crosslinking reaction. Finally, resuming water injection to crossflow from the high permeability zone into the less permeable zone. The subsequent water injection will flow with crossflow effect through the formerly unswept low permeability zones, resulting in increased oil production. The basic concept of gel placement is described in Fig. 1.

The use of seawater or partially desalinated seawater may be the only sustainable solution to prepare polymer solutions in some remote areas, especially at the offshore located in South East Asian countries, Arabian and Mexican Gulfs, and the North Sea. The effect of salinity on gelation performance of polymer gel is a noteworthy phenomenon. In fact, the oil business has started to embark on the research of salinity ranging more than 3.5%, the salinity of typical seawater [16-18]. Salinity is able to either accelerate or delay the process of gelation. Hypothetically, salinity does affect the hydrodynamic volume of the polymer, thus limiting the amount of accessible sites on the polymer and reducing the efficiency of NH_4Cl as retarder to delay gelation time [19,20]. Moreover, crosslinked polymer gels could have inadequate gel strength and shorter gelation time, especially at higher temperature. Therefore, additives are introduced to improve gel performance. For instance, high temperature reservoirs need gels with longer gelation time in order to prevent premature gelation and to ensure deep penetration of the injected gelant into the desired zone. Otherwise, gels can form inside tubing and lead to severe plugging problems. Based on field trials, practical gelation time should be more than 1 hour [21].

To tackle this issue, researchers over the past several years have

proposed the optimum concentration of retarders to improve gelation time [22]. The retarder affects the crosslinking reaction, thus prolonging the time in forming the gel. It is also thought that delaying gelation is more efficient by retardation on polymer compared to on crosslinker side [20]. In this case, NH_4Cl has been chosen as a retarder to increase the gelation time of PAM/PEI polymer gel for high temperature conformance control. The use of NH_4Cl as a retarder of polymer gel for high temperature application was patented by Al-Muntasheri et al. [23]. It is believed that retardation mechanism of NH_4Cl is by charge shielding effect on carboxylate groups along polymer chains. Thus, it reduces the reaction opportunity between polymer and cross-linker [24,25].

The addition of silica nanoparticles is also exhibited as an uncomplicated and economical solution as additive for polymer gel. Liu et al. studied the influence of silica nanoparticles on the gelation behavior of HMTA-HQ crosslinked polymer gel [26]. The result reveals that silica nanoparticles increase both elasticity and viscosity of the gel significantly. Its presence causes the rheological properties of the gel to be more solid-like, attributed to the hydrogen bonding between silica nanoparticles and polymer. In addition, silica nanoparticles aggregate themselves and form arrangements in a specific pattern during crosslinking reactions. The aggregation of nanoparticles normally takes place on polymer chain bunches and meshes of the gel structure. It contributes to significant improvement in gel strength. The presence of silica nanoparticles also improves the thermal stability of the gel. This is because of the water-lockup function associated with a large number of hydroxyl groups on the surface of silica nanoparticles [26].

In addition, silica nanoparticles also have negative charges in gelling solution. The hydroxyl groups form hydrogen bonds and electrostatic attractions with water molecules. It makes the water molecules to become bound water. Higher bound water ratio indicates stronger gel since it has better water holding capacity and thermal stability. Studies conducted with silica nanoparticles as additive also showed good results in improving salinity tolerance of the polymer gel as well. Metin et al. highlighted three approaches in the use of silica nanoparticles to strengthen polymer gels [27]. First, the silica is in the form of colloidal silica, which the suspension of fine amorphous, nonporous, and spherical silica particles is in the liquid phase, not as sodium silicate powder; second, gelation is controlled by salinity difference, instead of being triggered by the changes of pH; and finally, gelation happens at very low silica nanoparticle concentration.

The main objective of this paper is to present the core flooding experiments that have been used to evaluate the propagation of PAM/PEI polymer gels. In addition, the performance of various PAM/PEI polymer gels to block a high permeability zone and to divert the following water to a low permeability zone in porous media was also investigated. The work is based on four relevant elements that have to be considered to determine the suitability of a gel to mitigate excessive water problems in a high temperature and high pressure condition. They are adequate gelation time to achieve the target zone, reducing permeability to water, applicable injectivity, and long-term thermal stability [28].

EXPERIMENTAL APPROACH

1. Materials

The materials used in this study consist of polymer as main material, crosslinker and nanoparticles as solid filler. Other materials are sodium chloride (NaCl), which represents salinity and ammonium chloride (NH₄Cl) as retarder. The polymer used in this study is non-ionic Polyacrylamide (PAM) that was obtained from Sigma Aldrich. PAM is a straight chain polymer composed of acrylamide molecules of monomers. It is in granular form with pH 6 and was used as received without any further treatment. In this study, the molecular weight of PAM is on average 5,000,000–6,000,000 mol. wt. Meanwhile, Polyethylenimine (PEI) was used as a crosslinker provided by BASF with pH of approximately 11.7. The molecular weight and active content of PEI was 35,000 mol. wt. and 99%, respectively. It was accepted in liquid form and used without any further treatment for gel sample preparation. For salinity and retarder, NaCl and NH₄Cl were used, respectively. All of the salts were analytical reagents purchased from Sigma Aldrich with American Chemical Society grade. Deionized water was made in our labora-

tory. The silica-based nanoparticles (SiO₂ NP) were used as fillers to reinforce polymer gels in the present study. The size of silica NP used in this study is 5 nm, as stated by the supplier. The surface of the particle is spherical and solid without pores to ensure silica NP has adequate toughness.

2. Preparation of Polymer Solution

In this study, the samples of polymer gelants were prepared at room temperature by mixing 1.5 wt% of PAM and 0.3 v% of PEI. These concentrations of PAM and PEI are based on the formulation study by Amir et al. [29]. Hydrochloric acid (HCl) was used to neutralize the pH of the gelling solutions since the gelation process is optimum in neutral condition. The mixture was stirred using an IKA RW20 digital mixer at 200 rpm for an hour at room temperature. The time and speed of mixing of the sample were chosen to minimize the shear degradation in polymer gelant samples. Then, by maintaining the PAM/PEI ratio, the salinity, retarder, and solid additive, which have silica NP contents, were adjusted during preparation of polymer gels for further experimental work. For silica NP addition, nanoparticles were added with a required concentration before adding polymer and other materials. The experimental mixtures were stirred for 30 minutes. Then, an orbital shaker followed by an ultrasonic bath was utilized to ensure nanoparticles dispersed well and to avoid agglomeration.

3. Core Flooding Test

In this particular study, core flooding with crossflow effect using composite core that has permeability contrast was performed. The composite cores represent heterogeneous reservoirs. Four different sets of polymer gelant were prepared and then injected into the cores. The injection scenarios that have been performed in core samples are summarized in Table 1. These selected mixtures of gelant are sufficient to represent the effect of salinity, retarder, and solid nanoparticles on the gel in porous media.

4. Core Preparation

Berea sandstone core (Fig. 2(a)) was selected as porous media

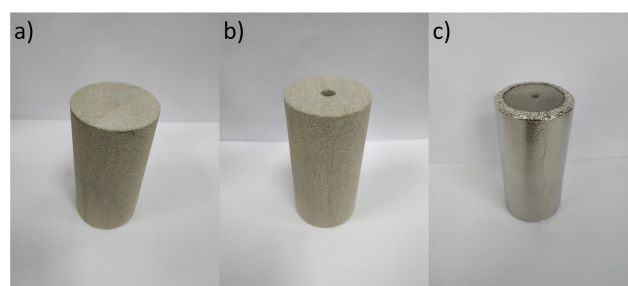


Fig. 2. Photo of (a) native core, (b) drilled core and (c) the core that has been sandpacked and wrapped with Nickel sheet.

Table 1. The core and injected polymer gelant

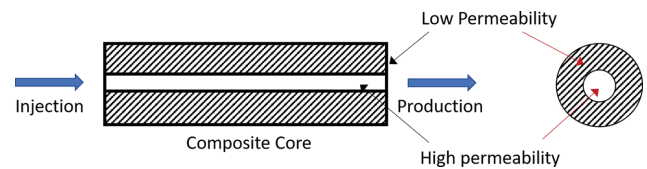
Core sample	Injected gelant
1	Pure PAM/PEI polymer gelant
2	PAM/PEI polymer gelant containing 5 wt% retarder
3	PAM/PEI polymer gelant containing 5 wt% retarder at 30,000 ppm salinity
4	Silica NP reinforced PAM/PEI polymer gelant containing 5 wt% retarder at 30,000 ppm salinity

Table 2. Petrophysical properties of cores used for coreflooding test

Core	Length (cm)	Diameter (cm)	Weight (gram)	Porosity (%)	K_{air} (mD)
1	7.576	3.83	181.76	20.605	341.113
2	7.438	3.828	177.755	20.881	347.097
3	7.66	3.83	184.428	20.192	340.836
4	7.49	3.83	180.27	20.31	356.785

to perform core flood experiments. The approximate dimensions of the core are 3.8 cm (1.5 inch) in diameter and length of 7.6 cm (3 inch). Four Berea core plugs with a range of permeability from 300 to 350 mD were used. All cores were cut from the same block. All cores are from outcrop (open cut mines) rocks containing no oil. The cores were extracted using a drilling core sampling apparatus. The extracted outcrop cores were dried in a hot oven at 100 °C for 24 hours until their weight was stable. The dry weight, length and diameter of cores were measured. Then, porosimeter and permeameter (Poroperm) were used to measure porosity and gas permeability, respectively. The measured dimensions and average petrophysical properties at initial condition are listed in Table 2.

To prepare the core as a composite core with crossflow effect, the configuration of 6 mm diameter cylindrical hole was drilled longitudinally through its center along the axis as shown in Fig. 2(b) and schematic diagram in Fig. 3. After the coaxial hole was drilled, sand was filled into the drilled part. The cores were wrapped tightly with nickel sheet, and wire screens were also put at both ends of the core as shown in Fig. 2(c). This sand-filled layer represents a high permeability layer, while the original sandstone layer represents a low permeability zone. The purpose of this setup is to

**Fig. 3. Schematic diagram of drilled core side view from side view (left) and front view (right).**

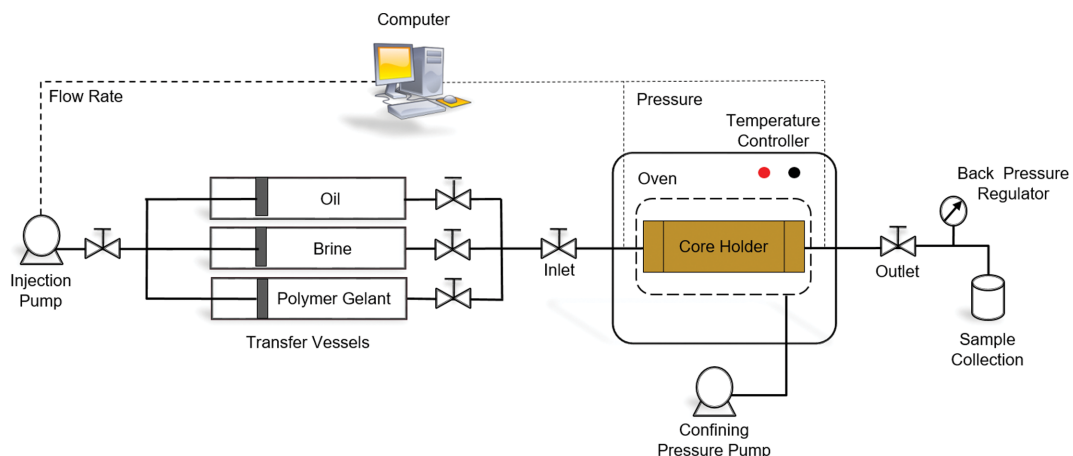
create capillary communication between low permeability (core) and high permeability (sand) layers. This is to simulate the cross flow effect across parallel layers by flooding fluid or water flooding in reservoirs. Then, the weight, diameter, length, permeability, and porosity of the composite cores were measured again. The measured dimensions and properties of the prepared composite cores are shown in Table 3. Finally, the cores were saturated with brine (30,000 ppm of NaCl) using a manual saturator under 1,000 psi of pressure condition. The saturation procedure is based on American Petroleum Institute standard (API RP 40).

5. Core Flooding Setup

The schematic diagram and photo of core flood set-up to exam-

Table 3. Petrophysical properties of the prepared composite cores used for coreflooding test with crossflow effect

Core	Length (cm)	Diameter (cm)	Weight (gram)	Porosity (%)	K_{air} (mD)
1	7.73	3.862	187.111	21.57	2685.088
2	7.562	3.85	183.281	22.288	2675.079
3	7.842	3.862	189.932	21.409	2755.703
4	7.63	3.86	185.543	21.513	2568.309

**Fig. 4. Schematic diagram of the coreflooding set-up.**

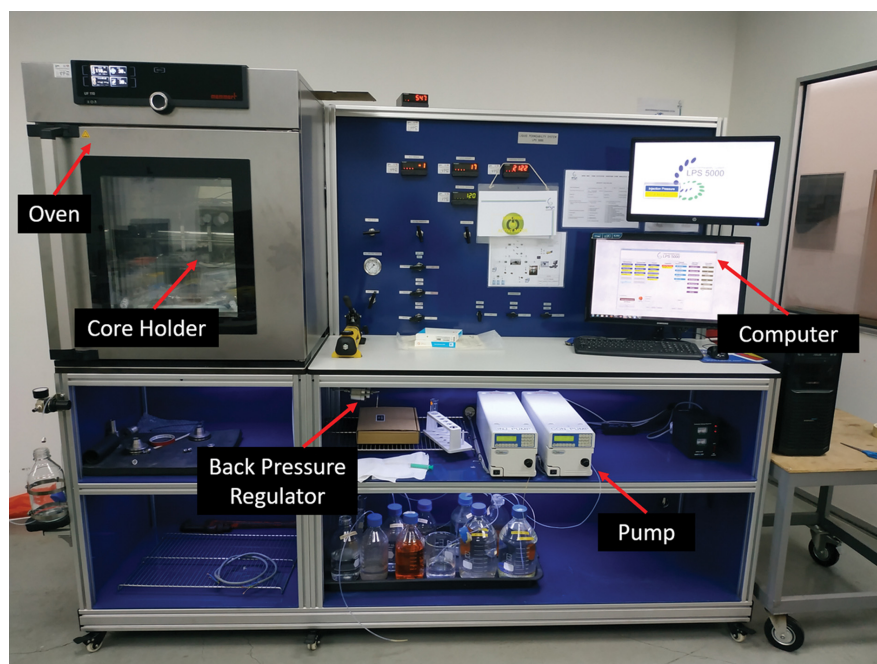


Fig. 5. Photo of the coreflooding set-up.

ine the blocking ability of the PAM/PEI gels in porous media are illustrated in Fig. 4 and Fig. 5, respectively. The main components of the experimental setup include a core holder designed to simulate reservoir rock and fluid flow, a constant rate HPLC pump for injecting oil, brine and polymer gelant. Core flooding experiments were conducted in a triaxial core holder made from a stainless steel (SS316L) cylinder. The core holder is placed inside an oven for high temperature exposure. Moreover, the pressure transducers are connected to the inlet and outlet ends of the core holder to measure and record the pressure drop or differential pressure along the core during the flooding process. The output from transducers then is transferred as pressure reading to the computer. The computer is also communicating with the pump to record the data of injection pressure, cumulative injected volume, and flow rate as a function of time. All data is viewed in real time and collected to a datasheet.

6. Core Flooding Procedure

The core was mounted into a core holder that was already placed in a convection heating oven having accuracy of ± 1 °C. The displacement tests were performed at constant temperature of 120 °C. The confining pressure of 2,000 psi was applied. The injection flow rate and injection pressure of the fluids was maintained at 0.5 cm³/min and 1,500 psi, respectively. The injection flow rate was selected as it is within the range of shear rates typically applied in water flooding operations in the field. A back-pressure of 1,500 psi was applied. Besides, as a balance for injection pressure, another purpose of the back pressure is to avoid evaporation of the liquids. It is connected to a data acquisition system that is capable of recording data points of all parameters for every 30 seconds. After the cores were mounted in the core holder, displacement tests with crossflow effect were performed in sequential flooding. First, brine was injected at different flow rates to measure the absolute perme-

ability of the core. It was measured using Darcy's law for linear flow:

$$K = \frac{Q\mu L}{A\Delta P} \quad (1)$$

where K is the permeability in mD, Q is the volumetric flow rate in cm³/min, μ is the brine viscosity in mPa-s, L is the core length in cm, A is the cross-sectional area available for flow in cm², and ΔP is the differential pressure across the core in psi.

This first brine injection is also to reach the initial water saturation (S_{wi}). It is followed with paraffin oil to displace water until no water comes out. The original oil-in-place (OOIP) was calculated based on the volume of water displaced. This is to establish initial oil saturation (S_{oi}). For the first cycle of oil recovery, brine is injected into the core plugs until oil production surely stops or 100% water cut. The residual oil saturation (S_{or}) is established due to first waterflooding (WF1). The core was continuously flooded with various prepared PAM/PEI polymer gelants as conformance control mode.

After the injection of polymer gelants, the core was shut-in for three days to allow the gelling up process. Following gelation, post-treatment water flooding was conducted and the volume of produced oil was determined. The displaced oil from the core was collected and measured during the displacement processes to evaluate the oil recovery performance (% of OOIP). Through the injection processes, the differential pressure with time was also recorded. The post-gelation average core permeability was also determined and the permeability reduction, k_R was calculated using the following equation:

$$k_R = \frac{k_i - k_a}{k_i} \times 100 \quad (2)$$

Where k_i is the permeability of the core to brine before the treat-

ment, and k_a is the permeability of the core after the gel treatment.

Finally, all of the core plugs were cut to observe the gelling profile.

RESULTS AND DISCUSSION

To study the performance of various PAM/PEI polymer gels in blocking and diverting the flow of water, a core flooding experiment with crossflow effect was conducted. Crossflow can occur to some extent in most reservoirs due to the heterogeneity of the reservoir. Successful conformance control by polymer gel is determined by placing blocking agent selectively in the high permeability layer and deep in the reservoir. After the gel is formed, the conduit is accessible for water to crossflow from the high permeability region into low permeability region. Thus, sweep efficiency can be improved.

The results of effective blocking and diverting water flow could produce higher oil recovery from the trap zone. To perform this experiment, on top of the tested gel, dye colored brine and paraffin oil were injected into layered composite cores with permeability contrast. The recovery includes water flooding (2 PV), then conformance control by polymer gel (1 PV), and finally water flooding after gel treatment (5 PV). Table 4 shows the cumulative oil recovery profile before and after conformance control with different formulation of PAM/PEI polymer gels. The cumulative oil recovery is the ratio of the produced oil to the original oil in place (OOIP) expressed as a percentage.

For the primary recovery process, it was conducted by waterflooding before gel placement. In general, as shown in Table 4 and Fig. 6, all of the cores apparently have an almost similar oil recovery during first brine flooding. Experimental results show that a significant amount of oil, around 40% of the OOIP, was produced after the initial recovery. Then, it means about another 60% of the oil still remained inside the core, assumed mostly in a low permeability area. To recover the remaining oil, gel placement followed by a subsequent cycle of waterflooding was carried out. However, during experimental work, only a small amount of oil was produced in the water flooding after gel treatment. Thereby, cumulative oil recovery is not an accurate criterion to determine the efficiency of polymer in diverting water flooding. Thus, it is crucial to compare the oil recovery after gel treatment instead of the cumulative oil recovery performance in determining the effectiveness of each gel plugging.

For secondary oil recovery, waterflooding was performed after the gelation process completed. Fig. 6 shows the performance of waterflooding for oil recovery after conformance control using various PAM/PEI polymer gels. As can be seen in Fig. 6, the oil pro-

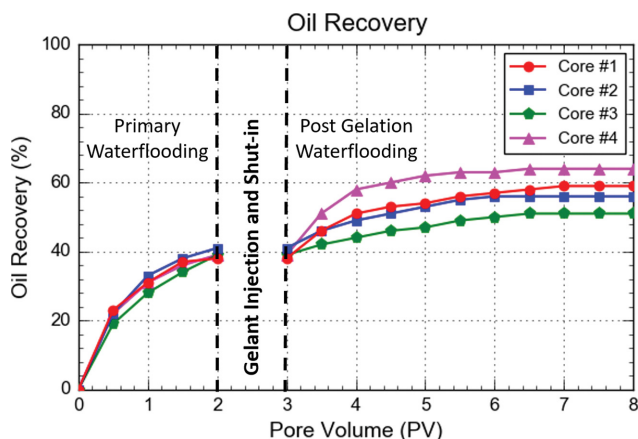


Fig. 6. The results of oil recovery versus pore volume for different cores treated with different PAM/PEI polymer gels.

duction is obviously higher during the first 1.5 PV of waterflooding after gel plugging. The relatively more oil recovery suggests the effectiveness of the polymer gel in diverting water flooding, than to sweep the trapped oil in low permeability area. Among the four tested polymer gels, two cores showed the produced oil less than 15% of OOIP as the result of post-gelation waterflooding. The two cores are the core #2 and core #3, which are treated with PAM/PEI polymer gel in 5 wt% NH_4Cl and with PAM/PEI polymer gel containing 5 wt% NH_4Cl in high salinity, respectively. For core #2, the cumulative oil recovery increases to 56% of the OOIP, so only 15% of the trapped oil was recovered by post-gelation water flooding. The scenario seems to have become worse when retarder was added into the gel that was prepared with high salinity brine. Lower oil recovery is observed after the treatment by this gel as can be seen in core #3. The cumulative oil recovery resulted in 51% of the OOIP. From this result, the post gelation oil recovery dropped to only 12%. It signifies the less effectiveness of polymer gel containing retarder in high salinity to block and divert the flow of water into low permeability layer. This is most probably due to lower strength of the formed gel. As 'fluid-like' gel has been washed out during waterflooding, water bypasses some areas of low permeability zone. Instead of brine being diverted to the low permeability zone, a flow path of brine is initiated within the high permeability area. It resulted in some amount of the trapped oil being untouched and unable to be swept out for the production.

Another two cores, core #1 and core #4, show considerably higher oil recovery. These two cores are the cores treated with pure PAM/PEI polymer gel and treated with polymer gel reinforced with silica NP, respectively. For core #1, after injection of pure poly-

Table 4. Oil recovery results with conformance control using different PAM/PEI polymer gels

Core number	1	2	3	4
Original oil in place (OOIP), %	91	94	89	92
Oil recovery of waterflooding before gelation, %OOIP	38	41	39	39
Total oil recovery, %OOIP	59	56	51	63
Oil recovery of waterflooding after gelation, %OOIP	21	15	12	24

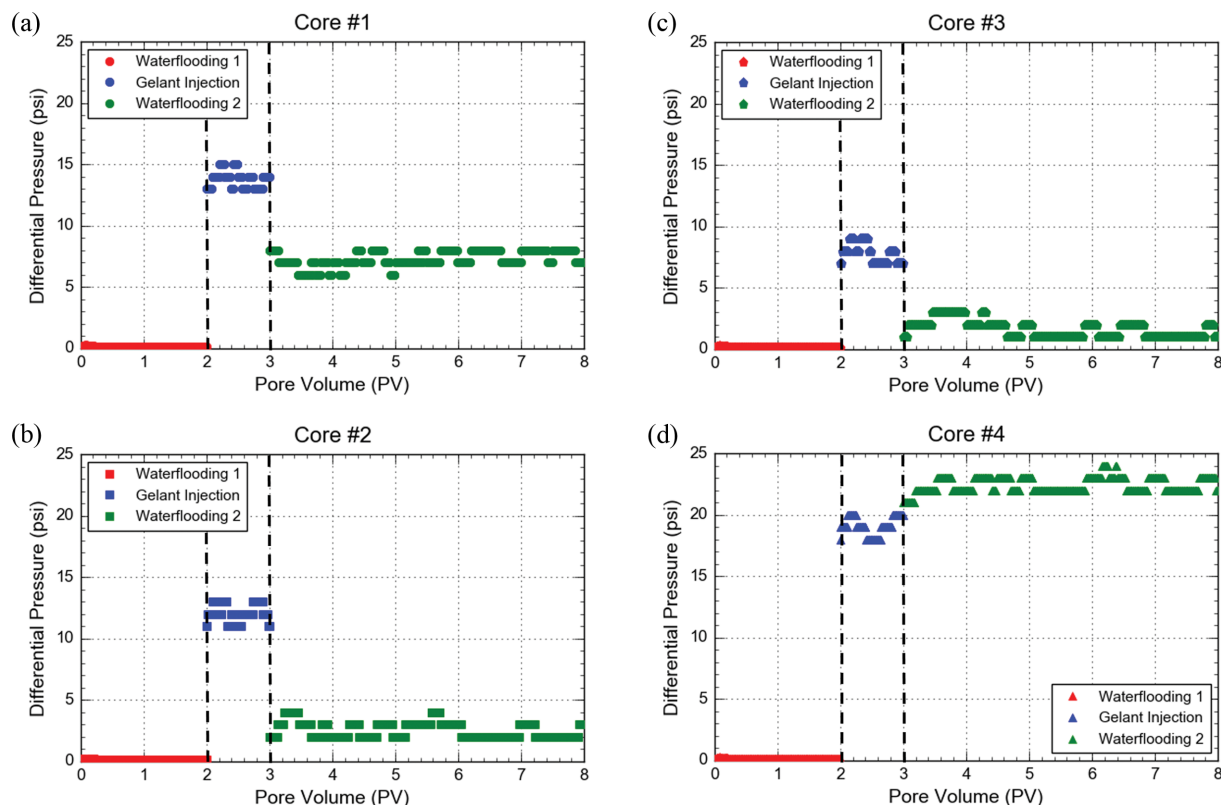


Fig. 7. Differential pressure as a function of pore volume in a coreflooding with crossflow effect experiments.

mer gelant and gelling up occurred, 21% of the remaining trapped oil was recovered by waterflooding. As a result, the cumulative oil recovery increased to about 59% of the OOIP. This result became the baseline for this experiment. On the other hand, higher oil recovery was established for core #4 that is treated with reinforced PAM/PEI polymer gel. In fact, the post gelation oil recovery for core #4 is the highest compared to the result of the other PAM/PEI polymer gels. As shown in Fig. 6 for core #4, the cumulative oil recovery increases to about 63% of the OOIP or 24% of the trapped oil recovered by waterflooding after reinforced gel treatment. This is about 3% additional oil being produced compared to the oil recovery after treatment using pure PAM/PEI polymer gel. Core treatment with reinforced polymer gel also doubles the amount of oil recovered from core treated with polymer gel containing retarder in high salinity. This indicates the advantage of silica NP reinforced PAM/PEI polymer gel to recover more trapped oil compared to PAM/PEI polymer gel without solid particles. It proves that silica NP reinforced polymer gel is capable of blocking, then diverting the flooding water and reaching the remaining oil, thus sweeping it efficiently. This is attributed to the higher gel strength of the formed gel. Efficient rigid gel makes less amount of the trapped oil unrecovered and left behind. Hence, it can be concluded that the addition of silica NP becomes the remedy to strengthen the polymer gel including the gel that has been weakened by salinity and retarder content.

Another important parameter to note in core flooding test is differential pressure data. The differential pressure or pressure drop across the core during the gelant injection and waterflooding of

brine is shown in Fig. 7. In the course of first brine flooding, the differential pressure is relatively similar for all of the cores. It shows that all of the composite cores have permeability in the same range. The results shown in Fig. 7 exhibit that the differential pressure is fairly stable at around 0.1 psi, corresponding to 2 PV of brine injection. This signifies that brine does not create a larger flow area through the porous medium leading to a stable differential pressure. In this case, the flow area of brine is mostly in high permeability sandpack. This differential pressure is immensely lower compared to the differential pressure as the result of post-gelation waterflooding as well. The absence of gel formation in high permeability zone of the core is the reason behind this observation.

Another pressure data that is significant to observe is differential pressure during gelant injection. Fig. 7 with blue marking shows the differential pressure during injection of 1 PV of various PAM/PEI polymer gelants. In general, the value of differential pressure increased during gelant placement in comparison with first brine injection. This is because gelant viscosity is higher than brine viscosity. Then, the differential pressure is greatly increased during waterflooding after gelation. The green marking in Fig. 7 indicates the differential pressure for waterflooding after gel treatment. Moreover, the discrepancy in differential pressure for different mixtures of polymer gelant is more obvious. As shown in Fig. 7(a), during injection of pure PAM/PEI polymer gel into core #1, the differential pressure increases to a maximum value of 13 psi. Then, the differential pressure decreases during waterflooding after gel treatment to around 8 psi. These pressure data become the benchmark for further core flooding test using different PAM/PEI polymer gels.

Meanwhile, during injection of PAM/PEI polymer gel with 5 wt% NH_4Cl gelant into core #2, the differential pressure across the core reaches a maximum of 11 psi as shown in Fig. 7(b). The injection pressure for the gel sample prepared with retarder is expected to be lower than the gel prepared with fresh water. The lower differential pressure during injection of gelant containing retarder is a noteworthy proof that gelant with retarder has lower viscosity. The fluid-like behavior of the gel can be ascribed to higher deformability as well. Gel deformability is related to the softness of the polymer gel. The gel in high salinity and retarder content has more deformability than the other gels. The softness or deformability of this polymer gel is proof that NH_4Cl has a greater effect on injectivity because the formed gel is softer and more deformable, thereby promoting lower injection pressure. Furthermore, the differential pressure of core #2 post-gelation waterflooding is around 3 psi, which is less than the acquired pressure data from waterflooding after gel treatment with pure polymer gel. This is due to lower strength of polymer gel with NH_4Cl ; the gel can be compressed and more microchannels are formed inside the porous media.

Then, further lower differential pressure can be seen when the injection of polymer gelant contains retarder in high salinity. This is based on the observation on the result from core #3 in Fig. 7(c). In fact, compared to the other treated cores, the lowest differential pressure during post-gelation waterflooding is noticed for the core treated with this gel. The differential pressure during injection and post-gelation waterflooding is around 8 and 3 psi, respectively. It indicates that it is easier to inject polymer gel prepared in high salinity into a core than the gel prepared in low salinity, but is not significantly effective in blocking and resisting the force of waterflooding. This trend is consistent with the findings regarding the low viscosity that contributes to higher injectivity. Also, this finding emphasizes that low gel strength contributes to high deformability of the gelant containing retarder in high salinity. This resulted in water that might have passed through the gel or flow within the high permeability zone bypassing the low permeability zone.

On the other hand, higher differential pressure data is collected from the core #4 that is treated with silica NP reinforced gel. As shown in Fig. 7(d), the observed differential pressure during gelant injection is around 18 psi. This higher differential pressure during injection is due to the higher viscosity of the gelant and higher gel flow resistance inside porous media. Moreover, the silica nanoparticle itself blocks the pore throats inside the core. Then, the differential pressure for the core #4 during waterflooding after gel treatment is about 21 psi. This is the highest differential pressure for post-gelation waterflooding that was recorded during this core flooding experiment. In fact, differential pressure was increased to achieve 24 psi at its maximum. It shows the high efficiency of reinforced gel in blocking the pore network in a high permeability area. This blocking is efficient as more rigid gel is formed inside porous media. The rigid reinforced gel is able to withstand the high pressure from water force, thus resulting in good diversion of water flow inside composite Berea sandstone cores. The essential conclusion from this particular study is that the solid particles are needed to strengthen the polymer gel.

Another important observation in conformance control that is associated with polymer gel is significant, leading to permeability

Table 5. Permeability reduction during conformance control by various PAM/PEI polymer gels

Core	Permeability reduction (%)
1	98.427
2	94.492
3	92.632
4	99.523

reduction in porous media. This reduction in permeability is due to the polymer gel presence inside the reservoir matrix. A measure of the polymer gel induced permeability reduction is the residual resistance factor, RRF, and it represents the reduction in the permeability of water as a result of gel. As presented in Table 5, the RRF trend is high for all cores plugged with all tested PAM/PEI polymer gels. As the RRF is higher, the PAM/PEI polymer gel is effective in plugging and impairing rock properties inside porous media. Higher RRF value increases the tendency of polymer gel to block high permeability zones, consequently diverting the waterflooding to the oil trapped zone. RRF can be calculated and signified through the discrepancy in differential pressure during waterflooding before and after polymer gelation.

As presented in Table 5, RRF value for the core #1 that is treated with pure PAM/PEI polymer gel is 98.43%. The value is calculated from the difference of differential pressure across the core during waterflooding before and after gelation that is increased from 0.1 to 8 psi. Then, RRF seems to decrease as retarder in the prepared polymer gel increases. For core #2 treated with PAM/PEI polymer gel with 5 wt% NH_4Cl as retarder, the RRF value is considerably decreased to 94.49%. This is because differential pressure for the two cycles of waterflooding is 0.1 and 3 psi, respectively. RRF for core #2 is apparently lower compared to the RRF of core #1 which is treated by pure PAM/PEI polymer gel. This is due to the lower gel strength. As injection water broke through the weak polymer gel, it initiated several microchannels and new water paths that allowed water to flow. These channels contribute to the reduction in RRF. Subsequently, the RRF is found to decrease further for core #3, which is after the gelation of PAM/PEI polymer gelant with 5 wt% retarder at 30,000 ppm salinity inside the core. The RRF value decreases further to 92.63%. This value is the lowest RRF value compared to other tested cores. It means the polymer gel containing retarder in high salinity has the lowest gel strength and is less effective in inducing reduction in permeability compared to the gel in core #2. The fact is microchannels formed within the gel structure are more severe. This is ascribed to the gel containing retarder in high salinity as the weakest gel compared to the other studied gel.

On the other hand, the highest RRF is found in core #4. After gelation of polymer gelant containing high salinity, retarder, and silica NP, the RRF value of core #4 increases to about 99.52%. This RRF value is about 7% more than polymer gel without silica NP. The RRF increased with the presence of solid filler in polymer gel, indicating a greater reduction in water permeability. It seems the high permeability zone has been blocked properly by the reinforced polymer gel. Less, or almost no, microchannel is created within gel network structure. In fact, reinforced polymer gel will be selectively placed in the high permeability area when treating confor-

mance problems. In addition, silica nanoparticles might be deposited and have a tendency to be retained inside the pore network of the core. Consequently, contributing to impairing the permeability and shutting-off water in high permeability zones. With fewer water channels in the high permeability zone, the resistance force for brine injection should increase. Then the water will be forced to flow to the low permeability zone where remaining oil is located.

Gel placement and water flow in porous media was visualized through observation of the dye stain inside the core. The brine for waterflooding was dyed to visualize the water flow. In this case, the treated cores were cut to four parts as shown Fig. 8, hence five surfaces were obtained for observation. The dye stain on the surface of the core cuttings was observed and the images of observation are presented in Fig. 9 to Fig. 12. When brine is injected, the

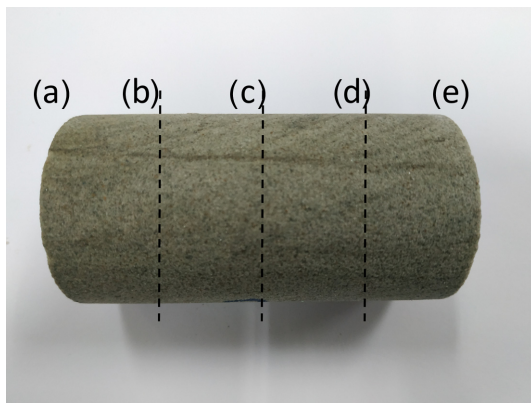


Fig. 8. Image of the cutting points for the tested cores.

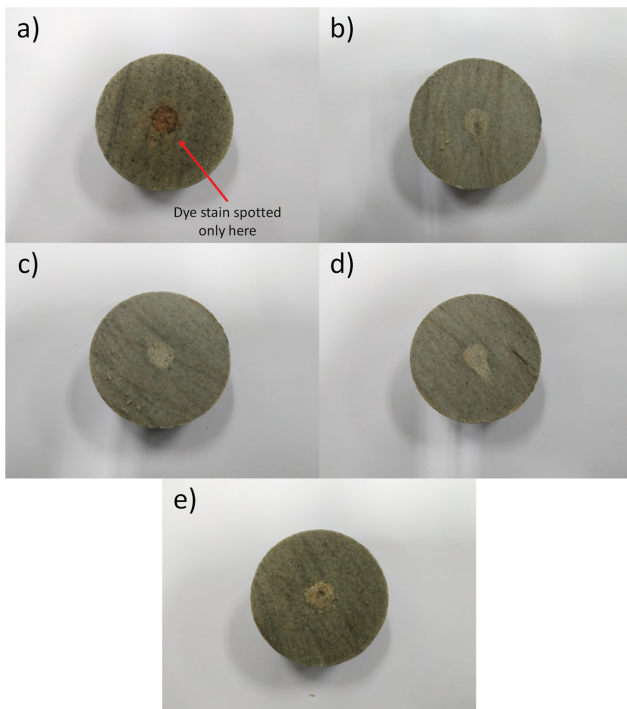


Fig. 9. Images of the cut core #1 that treated with pure PAM/PEI polymer gel.

dye stain will be left on the path of injection water flow. In general, a dye stain is only spotted on the inlet of the core, while not spotted on the outlet of the core. This shows that a rigid gel is formed inside the core. This gel is able to divert injection water; thus the brine did not discharge through the sandpack region. As observed in Fig. 9, for core #1, after the treatment using pure PAM/PEI polymer gel, a dye stain is observed on surface A. Meanwhile, no stain is seen from surface B onwards. This indicates the brine might be only able to travel at one-fourth of the core before it is blocked and diverted into a relatively higher permeability zone. Only a small amount of pure PAM/PEI polymer gel is washed out from the core due to the significantly higher strength of gel to resist the force of water. As the strong gel contained in porous media, the brine bypasses the gel unaffected and is diverted to the rock in the low permeability zone.

The same observation is seen from core #4, where the shortest distance of water travel is observed for the core treated with silica NP reinforced polymer gel. As shown in Fig. 12, for the core treated with reinforced gel, the dye stain is only spotted on the inlet of core or surface A. This rigid gel is able to divert injection water to the low permeability zone before water reaches surface B of the core. Thus, rigid gel has been formed and remained firm at the most part of high permeability streak. This indicates high strength of the reinforced gel. Silica NP as solid filler in polymer gel provides strong gel that eventually is able to withstand water force, washing out and gel compression. Hence, it signifies the effectiveness of silica NP to strengthen the weakened polymer gel for conformance control and increase the recovery of the trapped oil. Finally, brine has been observed to travel at a longer distance for the cores treated with gel containing NH_4Cl and in high salinity,

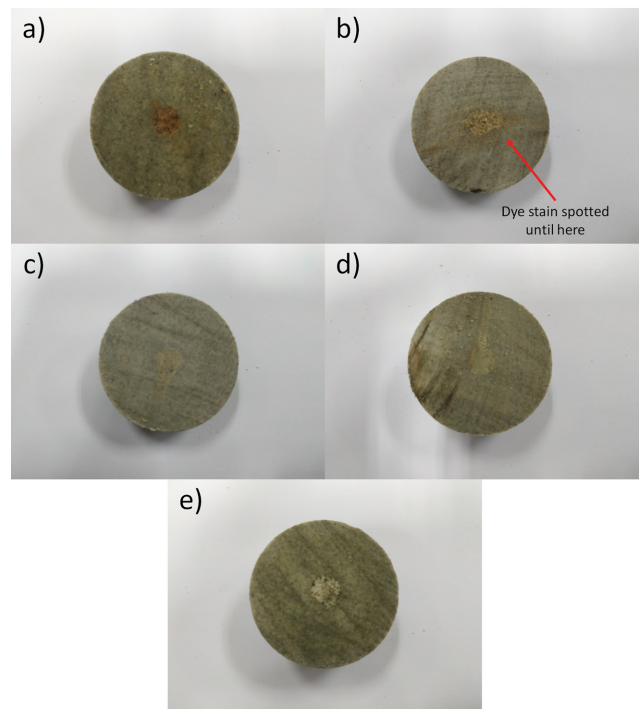


Fig. 10. Images of the cut core #2 that treated with PAM/PEI polymer gel containing 5 wt% NH_4Cl .

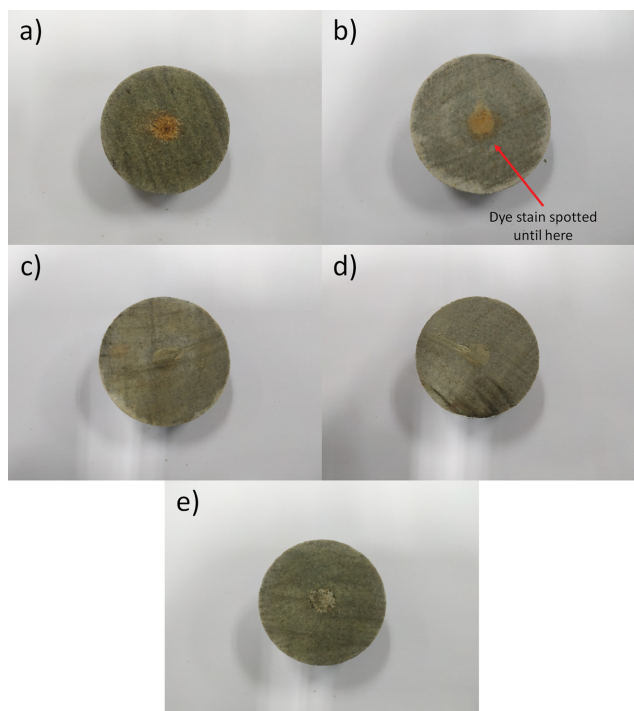


Fig. 11. Images of the cut cores #3 that treated with PAM/PEI polymer gel containing 5 wt% NH_4Cl in high salinity (30,000 ppm).

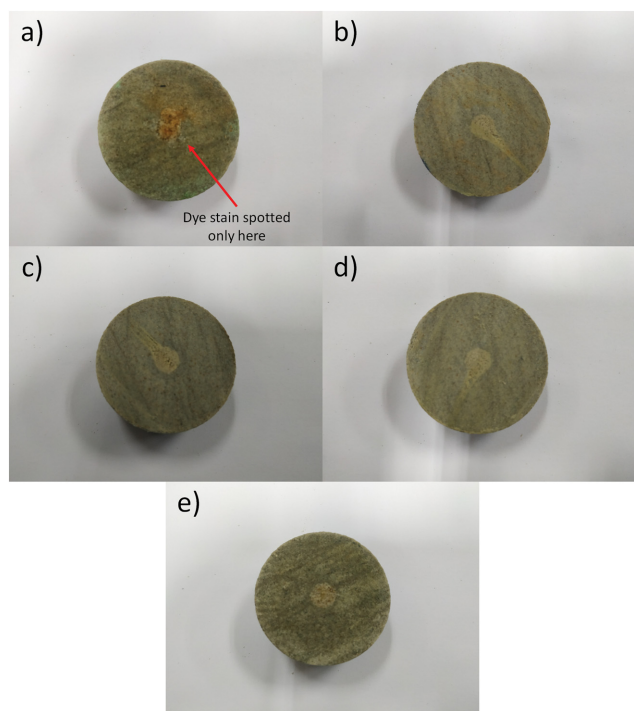


Fig. 12. Images of the cut core #4 that treated with silica NP reinforced PAM/PEI polymer gel containing 5 wt% NH_4Cl in high salinity (30,000 ppm).

without any filler. This can be seen at cores #2 and #3 as presented in Fig. 10 and Fig. 11, respectively. For cores #2 and #3 that are

treated by above-mentioned gels, dye stain is spotted until surface B of the cores. It is more than one-fourth of the high permeability zone reached by the brine before the diversion occurs. These observations indicate that gel has been washed out by brine. However, gel is not displaced completely. This indicates the low ability of the gels with high salinity and retarder to resist the water from traveling further in high permeability zone. This is due to the low strength of the gel structure.

CONCLUSIONS

It can be concluded that PAM/PEI polymer gel is effective in diverting injection water with crossflow effect to low permeability zone. For a study in porous media, the differential pressure can be used as an indication of the strength of gel in blocking the water in porous media. In general, with crossflow effect, the highest differential pressure can be observed in the core treated with silica NP reinforced PAM/PEI polymer gel. On the other hand, the lowest differential pressure is denoted when the treatment by polymer gel containing retarder in high salinity. In fact, the rigid reinforced gel is able to withstand the high pressure from water force, thus resulting in good diversion of water flow inside composite Berea sandstone cores. In addition, the core treated with polymer gel reinforced with silica NP yields considerably higher oil recovery up to 24% and permeability reduction. This shows the advantage of silica NP reinforced PAM/PEI polymer gel that tends to recover more trapped oil compared to PAM/PEI polymer gel without solid particles. In conclusion, the solid particle is needed to strengthen the polymer gel. In fact, the addition of silica NP becomes the remedy to strengthen the polymer gel, including the gel weakened by salinity and retarder content.

ACKNOWLEDGEMENT

The authors appreciate the contributions and financial supports from University of Malaya (IF062-2019), University of Malaya (FP050-2019A), Universiti Teknologi PETRONAS (YUTP 0153AAH05), Mr. Mohd Riduan Ahmad from Polygon Scientific Sdn. Bhd. and SLAI Fellowship Scheme from Ministry of Education Malaysia and University of Malaya.

CONFLICTS OF INTEREST

The authors declare that they have no conflict of interest.

REFERENCES

1. Y. Liang, Y. Ning, L. Liao and B. Yuan, in *Formation damage during improved oil recovery*, Elsevier (2018).
2. L. Nabzar, in *Panorama 2011: Water in fuel production-Oil production and refining*, Institut Francais du Petrole (IFP), France (2011).
3. J. Parshall, S. Whitfield and T. Jacobs, *J. Pet. Technol.*, **69**(5), 22 (2017).
4. J. Zheng, B. Chen, W. Thanyamanta, K. Hawboldt, B. Zhang and B. Liu, *Mar. Pollut. Bull.*, **104**(1-2), 7 (2016).

5. R. D. Sydansk and L. Romero-Zerón, in *Reservoir conformance improvement. society of petroleum engineers*, Richardson, Texas (2011).
6. D. Borling, K. Chan, T. Hughes and R. Sydansk, *Oilfield Rev.*, **6**(2), 44 (1994).
7. R. S. Seright, *SPE Prod Facil*, **10**(4), 241 (1995).
8. R. S. Seright and R. Lee, SPE Permian Basin Oil and Gas Recovery Conference (1998).
9. R. D. Sydansk and R. S. Seright, *SPE Prod Oper*, **22**(2), 236 (2007).
10. A. H. Kabir, SPE Asia Pacific Improved Oil Recovery Conference (2001).
11. A. Prada, F. Civan and E. D. Dalrymple, SPE/DOE Improved Oil Recovery Symposium (2000).
12. G. A. Al-Muntasheri, H. A. Nasr-El-Din, J. Peters and P. L. J. Zitha, *SPE J.*, **11**(4), 497 (2006).
13. Z. Amir, I. M. Said and B. M. Jan, *Polym. Adv. Technol.*, **30**(1), 13 (2019).
14. R. Seright, G. Zhang, O. Akanni and D. Wang, *J. Can. Pet. Technol.*, **51**(05), 393 (2012).
15. D. Wang and R. S. Seright, *Pet. Sci.*, **18**(04), 1097 (2021).
16. H. Zhao, P. Zhao, B. Bai, L. Xiao and L. Liu, *J. Can. Pet. Technol.*, **45**(05), 49 (2006).
17. M. H. Sharqawy, J. H. Lienhard and S. M. Zubair, *Desalination Water Treat.*, **16**(1-3), 354 (2010).
18. J. Wang, A. M. AlSofi and A. M. AlBoqmi, SPE EOR Conference at Oil and Gas West Asia (2016).
19. P. Kujawa, A. Audibert-Hayet, J. Selb and F. Candau, *Macromolecules*, **39**(1), 384 (2006).
20. K. S. M. El-Karsani, G. A. Al-Muntasheri, A. S. Sultan and I. A. Hussein, *SPE J.*, **20**(5), 1103 (2015).
21. G. A. Al-Muntasheri, L. Sierra, F. O. Garzon, J. D. Lynn and G. A. Izquierdo, SPE Improved Oil Recovery Symposium (2010).
22. K. S. M. El-Karsani, G. A. Al-Muntasheri and I. A. Hussein, *SPE J.*, **19**(1), 135 (2014).
23. G. A. Al-Muntasheri, L. Sierra and A. Bakhtyarov, U.S. Patent, US20140224489A1 (2014).
24. J. Kherb, S. C. Flores and P. S. Cremer, *J. Phys. Chem.*, **116**(25), 7389 (2012).
25. Z. Amir, I. M. Saaid, B. M. Jan, M. Khalil, M. F. A. Patah and W. Z. W. Bakar, *Polym. Bull.*, **77**(10), 5469 (2020).
26. Y. Liu, C. Dai, K. Wang, C. Zou, M. Gao, Y. Fang, M. Zhao, Y. Wu and Q. You, *Energy Fuels*, **31**(9), 9152 (2017).
27. C. O. Metin, K. M. Rankin and Q. P. Nguyen, *Appl. Nanosci.*, **4**(1), 93 (2014).
28. G. Zhao, C. Dai, A. Chen, Z. Yan and M. Zhao, *J. Pet. Sci. Eng.*, **135**, 552 (2015).
29. Z. Amir, I. Mohd Saaid and B. Mohamed Jan, *Int. J. Polym. Sci.*, Article ID 2510132 (2018).